

Effect of Multi-Pass Bending Deformation on Microstructure Evolution and Mechanical Properties of AZ31 Alloy Sheet

Qingshan Yang^{a,b*}, Zujian Yu^a, Qingwei Dai^a, Hanwu Dong^b and Bin Jiang^b

^aSchool of Metallurgy and Material Engineering, Chongqing University Of Science & Technology, Chongqing, 401331, China

^bChongqing Academy of Science and Technology – CAST, Chongqing, 401123, China

Received: April 22, 2015; Revised: November 30, 2015; Accepted: December 17, 2015

The rolled AZ31 Mg alloy sheets were processed by multi-pass bending (MPB) process at room temperature and followed by annealing treatment. Mechanical properties of the as-received and MPB sheets in annealed conditions were examined based on the concurrent microstructure and texture evolution. The results show that the room temperature ductility of the Mg sheets was improved by multi-pass bending process. Moreover, the (0002) basal texture was drastically weakened. Enhanced the ambient mechanical properties, such as lower yield strength and larger uniform elongation, were fabricated by MPB path due to the weak basal texture. The microstructure and mechanical responses were characterized and discussed.

Keywords: Mg alloy, Microstructure, Texture, Bending, Mechanical properties

1. Introduction

Magnesium (Mg) alloys have attracted considerable attention for a promising application in the automotive and electronics owing to their high specific strength and high electromagnetic shielding¹⁻⁵. However, the application of wrought Mg alloys has been limited by poor room temperature ductility^{6,7}. It was ascribed to the large difference in critical resolved shear stresses (CRSS) between basal and prismatic slip in hexagonal close-packed (*hcp*) crystal structure in Mg alloys⁸⁻¹². This results in a lack of the active slips systems and can hardly offer an arbitrary shape change at the grain level.

The plastic deformation modes of wrought Mg alloys depend on a combination of basal slip, non-basal slip and deformation twinning¹³⁻¹⁶. The basal slip is willingly to activate at room temperature because of the low CRSS¹⁷⁻¹⁹, which results in Mg alloy sheets show a strong (0002) basal texture after plastic deformation. Here, the *c*-axis of grains is predominantly aligned parallel to the normal direction (ND)^{20,21}. It has been reported that the ambient ductility of Mg alloy sheets strongly depends on the influence of the initial crystallographic texture of basal plane^{22,23}. This strong texture induces a poor deformation capability of sheet thinning and a stronger anisotropy, and consequently results in the low room temperature ductility. Thus, the texture control should be considered as an effective way to enhance the ductility in the following deformation processes at room temperature. In our work, the effect of multi-pass bending deformation on microstructure and mechanical properties of the rolled AZ31 alloy sheets was examined, which supplies a range of possible texture evolution to explore.

2. Experimental procedure

The material used in present work was commercially available wrought AZ31 (Mg–3% Al–1% Zn) rolled sheets with a thickness of 1 mm. Sheets were processed by the multi-pass bending (MPB) along the rolling direction (RD) at room temperature, as shown in Fig. 1. The device of MPB process was composed of up and down rollers. And the number of up and down rollers was 4, respectively. Here, the center of up and down rollers was not in a straight line, but rather to be staggered. Force of the sheets can be seen from Fig. 1(b). The rolling speed of MPB process was fixed at 5 m/min. The MPB sheets were then annealed at 300 °C for 1 h. The multi-pass bending and annealed sheets are referred to as MPBA sheets in the following paragraphs. The microstructure was examined by electron backscattered diffraction (EBSD) using HKL Chanel 5 System equipped FEI Nova 400 FEG-SEM. The X-ray texture analysis was carried out by Rigaku D/Max 2500.

Dumbbell tensile samples with nominal gage dimensions of 12, 6 and 1 mm were machined from the AZ31 sheets. Tensile tests were conducted on a CMT6305-300KN universal testing machine at the initial strain rate of 10⁻³ s⁻¹ at room temperature. The uniaxial tension was performed at the angles of 0°, 45° and 90° to the rolling direction. In the following paragraphs, RD, ND and TD represent the rolling, normal and transverse directions, respectively.

3. Results and discussion

The inverse pole figure (IPF) maps (ED-ND plane) of the as-received and MPBA sheets are shown in Fig. 2. It can be clearly seen from IPF maps that the grains of the MPBA sheets grew differently as compared to those of the

*e-mail: yangqsl@yeah.net

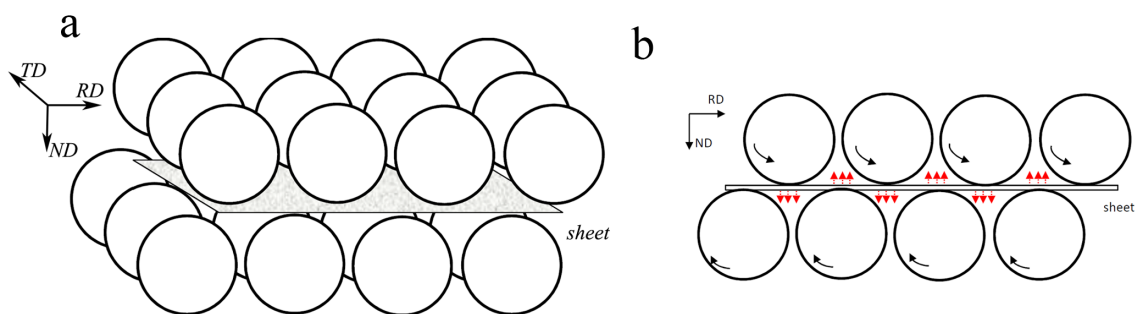


Fig. 1. (a) Schematic diagram of the multi-pass bending process. (b) Transverse section of multi-pass bending process in detail.

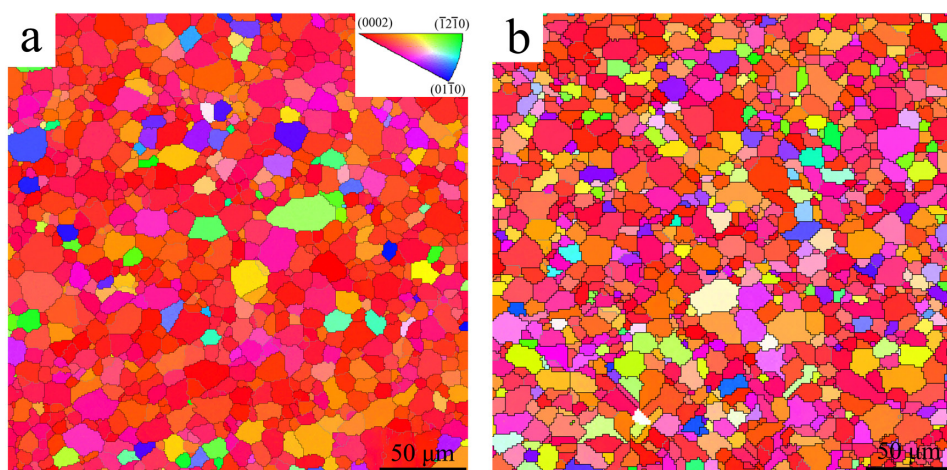


Fig. 2. EBSD results in IPF maps of (a) as-received sheets and (b) MPBA sheets.

as-received sheets. The microstructure of as-received sheet was homogeneous with equiaxed dynamically recrystallized (DRX) grains. In general, the red color expresses (0002) basal plane in *hcp* crystal structure, while the blue color represents the planes deviating 90° away from (0002) basal plane in IPF maps²⁴. As-received Mg alloy sheets exhibited the strong (0002) basal texture where $\langle 1120 \rangle$ direction in lots of grains orientated parallel to RD. After MPB process, the *c*-axis of grains mostly rotated away from the basal plane, which suggests that (0002) basal texture of MPBA sheets was relatively weakened. Thus, MPB process resulted in strong divergence of the grain orientation.

The grain size of AZ31 alloy sheets obtained from EBSD data is denoted in Fig. 3. As-received sheets were characterized by DRX grains of about $12 \mu\text{m}$. The average grain size of MPBA sheets was about $8 \mu\text{m}$. It can be seen that the fraction of large grains in MPBA sheets dropped sharply, as shown in Fig. 3(b). The MPB process is consisted of compress and shear deformation. This was introduced shear deformation into thin Mg alloy sheets between the upper and lower rollers. At the beginning stage of MPB process, when the Mg alloy sheets pass over first roller, it is very difficult to activate basal slip during bending because of the strong (0002) basal texture. Here, the plastic deformation mainly depends on the prismatic slip and the pyramidal twins. During the following rolling passes, the orientations

and stress states of the grains are changed because of the alternating operations of slip and twinning. Grain refinement mechanism was mainly due to grain subdivision in order to accommodate the intense plastic strain by the bending deformation. During the multi-pass bending process, the storage energy could drive the nucleation to finish the recrystallization. The growth continuously raised, and the increase in nucleation rate was higher than one in rate of the growth, resulting in a decrease in average grain size²⁵.

The fraction of boundaries as a function of the misorientation angle for adjacent grains of as-received and MPBA sheets was measured in Fig. 4. Grain boundaries in the IPF maps were indicated by various lines depending upon the grain-to-grain misorientation angles: gray for $2^\circ < \theta < 15^\circ$ (low-angle boundaries, LABs) and black for $15^\circ < \theta < 90^\circ$ (high-angle boundaries, HABs)²⁶. It can be seen that a higher density of low angle misorientations ($10^\circ \sim 40^\circ$) was in as-received sheets, while a higher density of high angle misorientations ($30^\circ \sim 90^\circ$) was in MPBA sheets. More random distribution of grain orientation can be obtained by MPBA process. Meanwhile, the recrystallization and nucleation of new grains during the MPB process were different from those of the parent grains at orientation angles.

To provide a full depiction of the basal texture and clearly represent its evolution during the MPB process, the pole figures of as-received and MPBA sheets are shown in

Fig. 5. The macrotexture texture of the as-received sheets exhibited a strong basal texture and ellipsoidal intensity distribution in the (0002) basal pole figure, as shown in Fig. 5(a). The MPB routes strongly affect the texture including the characteristics of the orientation distribution, the inclination direction of the basal plane and the texture intensity. Compared with the as-received sheet, the basal

texture of MPBA sheets was remarkably weakened. For Mg alloy with a *hcp* crystalline structure, the basal slip dominated the deformation at the low strain at room temperature^{27,28}. During the MPB process, the *c*-axes of the grains rotated to the TD–RD plane, which could be attributed to the basal dislocation activity in favorably oriented grains during the bending deformation. It was suggested that the majority of

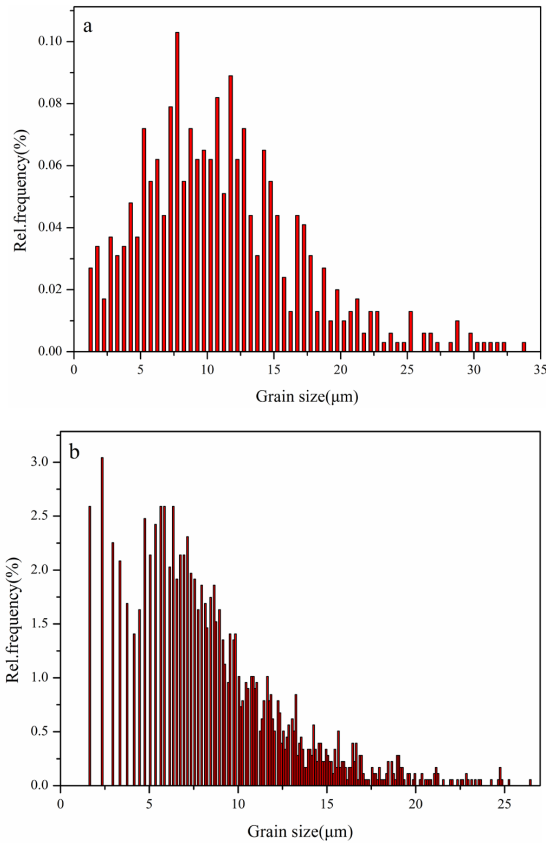


Fig. 3. The distribution of grain size of (a) as-received sheets and (b) MPBA sheets.

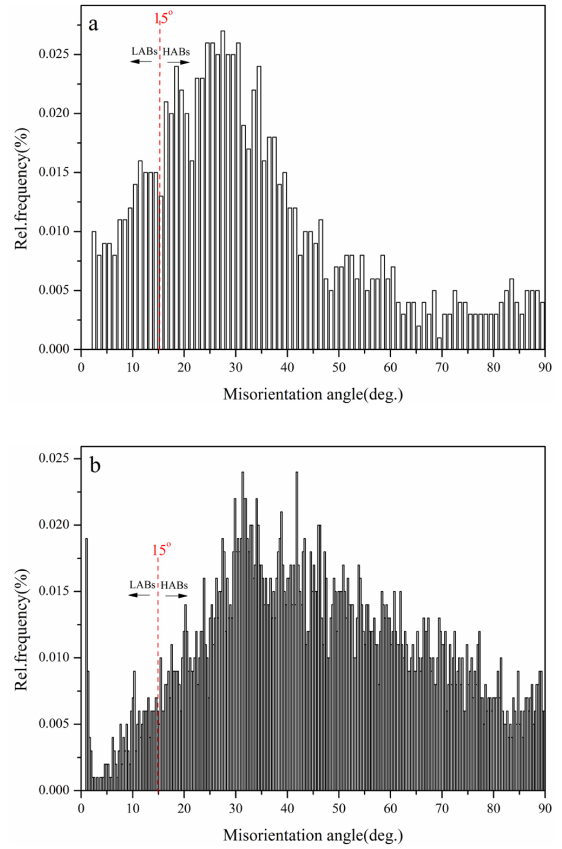


Fig. 4. The distribution of misorientation angle of (a) as-received sheets and (b) MPBA sheets.

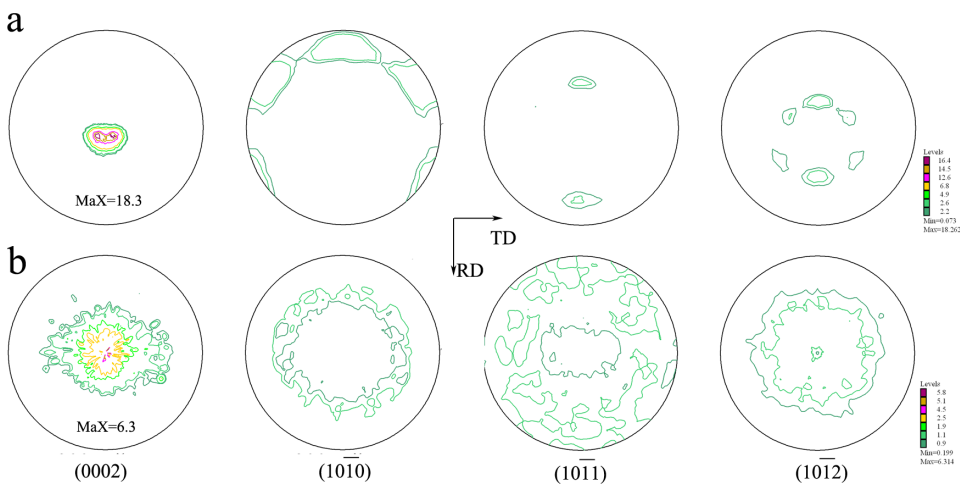


Fig. 5. The macroscopic texture of (a) as-received sheets and (b) MPBA sheets.

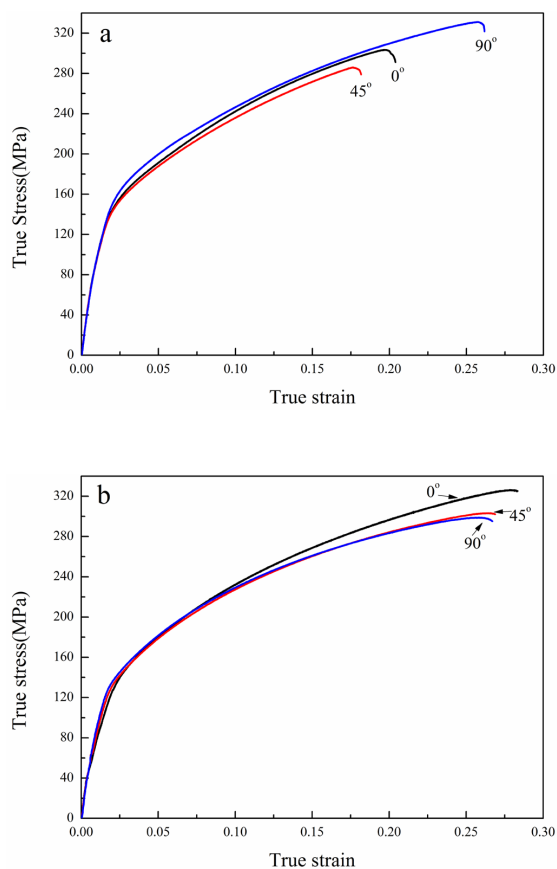


Fig. 6. The true train-stress curves of (a) as-received sheets and (b) MPBA sheets.

grains would be more suitable for prismatic $\langle a \rangle$ slip than basal $\langle a \rangle$ slip during bending deformation, and prismatic $\langle a \rangle$ slip was the major mode of strain accommodation^{29,30}

The true stress-strain curves of as-received sheets and MPBA sheets measured at different directions of 0°, 45° and 90° to ED at room temperature are depicted in Fig. 6. Mechanical properties, e.g. yield strength (YS, 0.2% offset strength), ultimate tensile strength (UTS) and uniform elongation (E_u) are also summarized in Fig. 7. It can be seen that the MPBA sheet exhibits superior room temperature ductility in every directions compared with as-received sheets. And MPBA sheets show lowest yield strength. In general, the Mg alloy with a strong basal texture would place many grains in hard orientations^{31,32}. The critical resolved shear stress (CRSS) of the (0002) basal slip is about 1/100 that of non-basal slip in Mg alloys, which leads to the stress localization and premature shear failure during the deformation process. With an increase in the basal Schmid factor and activation of the basal slip system, an angle is formed between the basal planes of the grains and the bending direction so that the c -axis becomes inclined from the ND towards the RD. Thus, it was suggested that the weaker (0002) basal texture could result in a higher Schmid factor of the basal slip and thus leads to the lower yield strength and higher ductility^{33,34}.

The plastic deformation at room temperature can be accommodated by the dislocation slip on the basal plane in

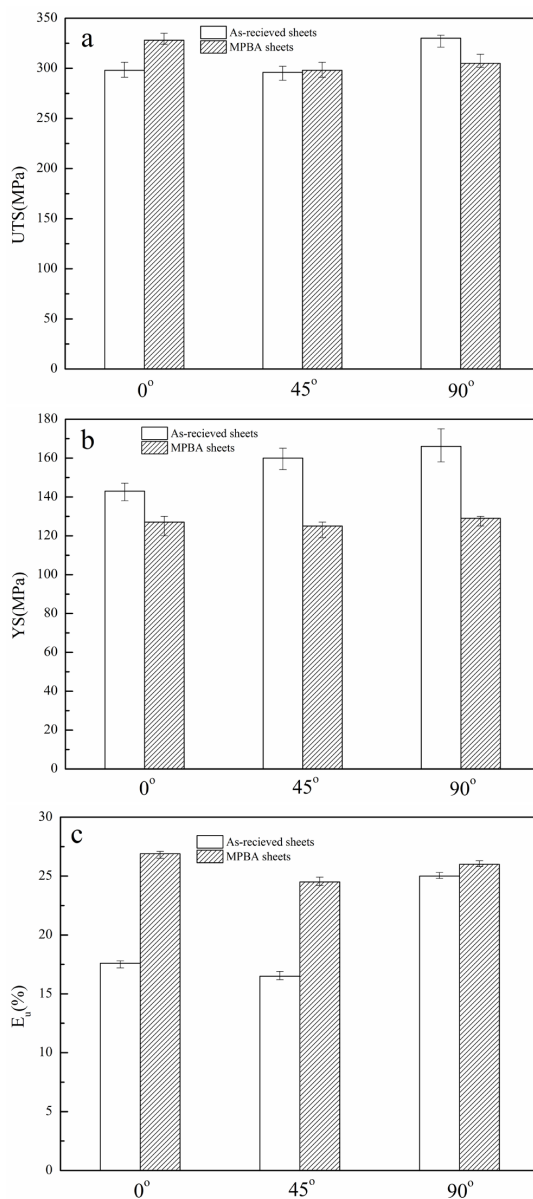


Fig. 7. Ultimate tensile strength (a), yield strength (b) and uniform elongation (c) of as-received and MPBA sheets.

Mg alloys^{35,36}. The as-received Mg alloy sheets with strong basal texture are unfavorable for basal slip during the plastic deformation. For MPBA sheets, the weak basal texture and inclination of the c -axes favor the action of basal slip during the deformation. During multi-pass bending deformation, repeated up-down bending gives rise to the waved strain. This could lead to the strong divergence of the grain orientation and triggered the angular spread of the (0002) basal plane, and thus favored the texture modifications.

4 Conclusions

In summary, we demonstrated that room temperature ductility of rolled AZ31 alloy sheets can be enhanced by employing a multi-pass bending process followed by

annealing. The divergence of grain orientation and weak basal texture were also obtained by MPBA process. Improved mechanical properties, such as lower yield strength and larger uniform elongation, were received in the direction of 0°, 45° and 90° to ED at room temperature compared with the as-received sheet. MPBA approach is an efficient alternative to improve the room temperature ductility of the rolled AZ31 alloy sheets.

References

- Luo AA. Magnesium casting technology for structural applications. *Journal of Magnesium and Alloys*. 2013; 1(1):2-22. <http://dx.doi.org/10.1016/j.jma.2013.02.002>.
- Kurukuri S, Worswick MJ, Bardelcik A, Mishra RK and Carter JT. Constitutive behavior of commercial grade ZEK100 magnesium alloy sheet over a wide range of strain rates. *Metallurgical and Materials Transactions. A, Physical Metallurgy and Materials Science*. 2014; 45(8):3321-3337.
- Agnew SR, Mehrotra P, Lillo TM, Stoica GM and Liaw PK. Crystallographic texture evolution of three wrought magnesium alloys during equal channel angular extrusion. *Materials Science and Engineering A*. 2005; 408(1):72-78. <http://dx.doi.org/10.1016/j.msea.2005.07.052>.
- Dai J, Jiang B, Li X, Yang Q, Dong H, Xia X, et al. The formation of intermetallic compounds during interdiffusion of Mg–Al/Mg–Ce diffusion couples. *Journal of Alloys and Compounds*. 2015; 619:411-416. <http://dx.doi.org/10.1016/j.jallcom.2014.09.071>.
- Yang Q, Jiang B, Jiang W, Luo S and Pan F. Evolution of microstructure and mechanical properties of Mg–Mn–Ce alloys under hot extrusion. *Materials Science and Engineering A*. 2015; 628:143-148. <http://dx.doi.org/10.1016/j.msea.2015.01.048>.
- Zhang H, Liu Y, Fan J, Roven HJ, Cheng W, Xu B, et al. Microstructure evolution and mechanical properties of twinned AZ31 alloy plates at lower elevated temperature. *Journal of Alloys and Compounds*. 2014; 615:687-692. <http://dx.doi.org/10.1016/j.jallcom.2014.07.045>.
- Huang G, Wang L, Zhang H, Wang Y, Shi Z and Pan F. Evolution of neutral layer and microstructure of AZ31B magnesium alloy sheet during bending. *Materials Letters*. 2013; 98:47-50. <http://dx.doi.org/10.1016/j.matlet.2013.02.055>.
- Roostaei AA, Zarei-Hanzaki A, Abedi HR and Rokni MR. An investigation into the mechanical behavior and microstructural evolution of the accumulative roll bonded AZ31 Mg alloy upon annealing. *Materials & Design*. 2011; 32(5):2963-2968. <http://dx.doi.org/10.1016/j.matdes.2011.01.038>.
- Huang X, Suzuki K, Chino Y and Mabuchi M. Influence of initial texture on rolling and annealing textures of Mg–3Al–1Zn alloy sheets processed by high temperature rolling. *Journal of Alloys and Compounds*. 2012; 537:80-86. <http://dx.doi.org/10.1016/j.jallcom.2012.05.002>.
- Qi F, Zhang D, Zhang X and Xu X. Effect of Sn addition on the microstructure and mechanical properties of Mg–6Zn–1Mn (wt.%) alloy. *Journal of Alloys and Compounds*. 2015; 585(5):656-666. <http://dx.doi.org/10.1016/j.jallcom.2013.09.156>.
- Min J, Hector LG, Lin J, Carter JT and Sachdev AK. Spatio-temporal characteristics of propagative plastic instabilities in a rare earth containing magnesium alloy. *International Journal of Plasticity*. 2014; 57:52-76. <http://dx.doi.org/10.1016/j.ijplas.2014.02.004>.
- Jiang Z, Jiang B, Yang H, Yang Q, Dai J and Pan F. Influence of the Al₂Cu phase on microstructure and mechanical properties of Mg–Al–Ca alloys. *Journal of Alloys and Compounds*. 2015; 647:357-363.
- Lee SY, Wang H, Gharghoury MA, Nayyeri G, Woo W, Shin E, et al. Deformation behavior of solid-solution-strengthened Mg–9 wt.% Al alloy: In situ neutron diffraction and elastic–viscoplastic self-consistent modeling. *Acta Materialia*. 2014; 73:139-148. <http://dx.doi.org/10.1016/j.actamat.2014.03.038>.
- Stanford N, Atwell D, Beer A, Davies C and Barnett MR. Effect of microalloying with rare-earth elements on the texture of extruded magnesium-based alloys. *Scripta Materialia*. 2008; 59(7):772-775. <http://dx.doi.org/10.1016/j.scriptamat.2008.06.008>.
- Molnár P, Ostapovets A and Jäger A. Reversible motion of twin boundaries in AZ31 alloy and new design of magnesium alloys as smart materials. *Materials & Design*. 2014; 56:509-516.
- Pan H, Qin G, Xu M, Fu H, Ren Y, Pan F, et al. Enhancing mechanical properties of Mg–Sn alloys by combining addition of Ca and Zn. *Materials & Design*. 2015; 83:736-744. <http://dx.doi.org/10.1016/j.matdes.2015.06.032>.
- Zhang Z. Twinning and its related work hardening during the ambient extrusion of a magnesium alloy. *Materials Science and Engineering A*. 2013; 577:125-137.
- Xin Y, Zhou X and Liu Q. Suppressing the tension–compression yield asymmetry of Mg alloy by hybrid extension twins structure. *Materials Science and Engineering A*. 2013; 567:9-13.
- He J, Jiang B, Yang Q, Li X, Xia X and Pan F. Influence of pre-hardening on microstructure evolution and mechanical behavior of AZ31 magnesium alloy sheet. *Journal of Alloys and Compounds*. 2015; 621:301-306. <http://dx.doi.org/10.1016/j.jallcom.2014.09.214>.
- Piao K, Lee JK, Kim JH, Kim HY, Chung K, Barlat F, et al. A sheet tension/compression test for elevated temperature. *International Journal of Plasticity*. 2012; 38:27-46.
- Yang Q, Jiang B, He J, Song B, Liu W, Dong H, et al. Tailoring texture and refining grain of magnesium alloy by differential speed extrusion process. *Materials Science and Engineering A*. 2014; 612:187-191. <http://dx.doi.org/10.1016/j.msea.2014.06.045>.
- Wang LF, Huang GS, Li HC and Zhang H. Influence of strain rate on microstructure and formability of AZ31B magnesium alloy sheets. *Transactions of Nonferrous Metals Society of China*. 2013; 23(4):916-922. [http://dx.doi.org/10.1016/S1003-6326\(13\)62548-0](http://dx.doi.org/10.1016/S1003-6326(13)62548-0).
- Huang X, Chino Y, Mabuchi M and Matsuda M. Influences of grain size on mechanical properties and cold formability of Mg–3Al–1Zn alloy sheets with similar weak initial textures. *Materials Science and Engineering A*. 2014; 611:152-161. <http://dx.doi.org/10.1016/j.msea.2014.05.083>.
- Hamad K, Megantoro RB and Ko YG. Microstructure and texture evolution in low carbon steel deformed by differential speed rolling (DSR) method. *Journal of Materials Science*. 2014; 49(19):6608-6619.

25. Stanford N, Geng J, Chun YB, Davies CH, Nie JF and Barnett MR. Effect of plate-shaped particle distributions on the deformation behaviour of magnesium alloy AZ91 in tension and compression. *Acta Materialia*. 2012; 60(1):218-228. <http://dx.doi.org/10.1016/j.actamat.2011.10.001>.
26. Li R, Pan F, Jiang B, Dong H and Yang Q. Effect of Li addition on the mechanical behavior and texture of the as-extruded AZ31 magnesium alloy. *Materials Science and Engineering A*. 2013; 562:33-38. <http://dx.doi.org/10.1016/j.msea.2012.11.032>.
27. Ghaffari Tari D, Worswick MJ, Ali U and Gharghoury MA. Mechanical response of AZ31B magnesium alloy: Experimental characterization and material modeling considering proportional loading at room temperature. *International Journal of Plasticity*. 2014; 55:247-267. <http://dx.doi.org/10.1016/j.ijplas.2013.10.006>.
28. Atwell DL, Barnett MR and Hutchinson WB. The effect of initial grain size and temperature on the tensile properties of magnesium alloy AZ31 sheet. *Materials Science and Engineering A*. 2012; 549:1-6. <http://dx.doi.org/10.1016/j.msea.2012.03.107>.
29. Zhang H, Huang G, Wang L, Roven HJ, Xu Z and Pan F. Improved ductility of magnesium alloys by a simple shear process followed by annealing. *Scripta Materialia*. 2013; 69(1):49-52. <http://dx.doi.org/10.1016/j.scriptamat.2013.03.011>.
30. Sankaran A, Madam SV, Nouri A and Barnett MR. Attaining high compressive strains in pure Mg at room temperature by encasing with pure Al. *Scripta Materialia*. 2012; 66(10):725-728. <http://dx.doi.org/10.1016/j.scriptamat.2012.01.041>.
31. Zhang H, Jin W, Fan J, Cheng W, Roven HJ, Xu B, et al. Grain refining and improving mechanical properties of a warm rolled AZ31 alloy plate. *Materials Letters*. 2014; 135:31-34. <http://dx.doi.org/10.1016/j.matlet.2014.07.130>.
32. Zhang H, Huang G, Fan J, Roven HJ, Pan F and Xu B. Deep drawability and deformation behavior of AZ31 magnesium alloy sheets at 473K. *Materials Science and Engineering A*. 2014; 608:234-241. <http://dx.doi.org/10.1016/j.msea.2014.04.081>.
33. Song B, Guo N, Liu T and Yang Q. Improvement of formability and mechanical properties of magnesium alloys via pre-twinning: A review. *Materials & Design*. 2014; 62:352-360. <http://dx.doi.org/10.1016/j.matdes.2014.05.034>.
34. Yang QS, Jiang B, Huang XY, Zhou GY, Dai JH and Pan FS. Influence of microstructural evolution on mechanical behaviour of AZ31 alloy sheet processed by flat extrusion container. *Materials Science and Technology*. 2013; 29(8):1012-1016. <http://dx.doi.org/10.1179/1743284712Y.0000000110>.
35. Doiphode RL, Narayana Murty SV, Prabhu N and Kashyap BP. Effects of caliber rolling on microstructure and room temperature tensile properties of Mg-3Al-1Zn alloy. *Journal of Magnesium and Alloys*. 2013; 1(2):169-175. <http://dx.doi.org/10.1016/j.jma.2013.07.005>.
36. Arab SM and Akbarzadeh A. The effect of Equal Channel Angular Pressing process on the microstructure of AZ31 Mg alloy strip shaped specimens. *Journal of Magnesium and Alloys*. 2013; 1(2):145-149. <http://dx.doi.org/10.1016/j.jma.2013.07.001>.